



Cu-state evolution during leaching of bornite at 50 °C

Cong-ren YANG, Fen JIAO, Wen-qing QIN

School of Minerals Processing and Bioengineering, Central South University, Changsha 410083, China

Received 3 April 2017; accepted 7 November 2017

Abstract: The bioleaching of bornite with mixed moderately thermophilic culture at 50 °C was investigated. The intermediary species formed during the leaching of bornite were characterized by XRD and XPS. In addition, the evolution of Cu-state during leaching of bornite was further studied by applying ϕ_h -pH diagram and cyclic voltammetry. The results showed that the bornite was more likely to be leached at high redox potential. Furthermore, the intermediary sulfides, such as isocubanite, covellite, chalcopyrite, disulfide, and polysulfide, were formed in the course of bornite dissolution. The Cu 2p photoelectron spectrum revealed that the valence of copper in bornite and intermediary sulfide formed in the dissolution of bornite is +1. The bornite and chalcopyrite can be converted into each other, and both can be further converted to covellite and/or chalcocite.

Key words: leaching; bornite; chalcopyrite; covellite; Cu-state evolution

1 Introduction

Bornite is an important source of copper. The oxidation state for copper in bornite is expected to be Cu(I), then the iron oxidation state would be Fe(III) [1–4], thus bornite can be written as $\text{Cu}^{\text{I}}_5\text{Fe}^{\text{III}}\text{S}_4$. However, MIKHLIN et al [5] argued that the total electron yield (TEY) Fe L 2,3-edge spectrum of bornite indicates some quantity of Fe(II) for bornite, and the composition of bornite can be written as $\text{Cu}^{\text{II}}\text{Cu}_4\text{Fe}^{\text{II}}\text{S}_4$, showing that copper in the mineral occurs in both monovalent and divalent states [2,6]. Many researchers have reported that bornite can form during the reduction of chalcopyrite at the cathode [7,8], while, MAJUSTE et al [9] stated that the bornite was detected on the surface of chalcopyrite after electrochemical oxidation in the potential window of 0.75 to 0.90 V.

A variety of bornite leaching experiments have been performed. Several researchers assumed that Cu dissolved preferentially from the bornite [9–12]. CuS and Cu_3FeS_4 were formed during the leaching of bornite with O_2 and H_2SO_4 [13]. BEVILAQUA et al [14] reported that a passive film formed on the surface of bornite, and the cyclic voltammetry results showed that

bornite was oxidized to a secondary CuS and reduced to non-stoichiometric copper disulfide intermediaries. Similarly, ZHAO et al [15] stated that bornite was directly oxidized to CuS and Cu^{2+} , and the formed CuS passivated the bornite. The oxidation of finely ground bornite by *Acidithiobacillus ferrooxidans* was evaluated in oxygen uptake and shake flasks experiments, covellite was detected as a secondary phase [16], and the bornite dissolution was accelerated by the adsorption of bacterial action on its surface [6,17]. ZHAO et al [18,19] reported that the addition of chalcopyrite accelerated the bioleaching of bornite. In addition, the gene and protein expression modulation methods by bornite in *Acidithiobacillus ferrooxidans* were also investigated. Although bornite had a slight impact on the expression of genes [20], it significantly altered in the level of protein expression [21].

The moderate thermophiles and extreme thermophiles microorganisms are widely used to leach metal sulfides with high efficiency [7,22–25]. Therefore, the aim of this study is to evaluate the bornite bioleaching by employing a mixed moderately thermophilic culture. The intermediary species formed in the leaching of bornite were characterized by XRD and XPS. Furthermore, the Cu-state evolution during

Foundation item: Project (2016RS2016) supported by the Hunan Provincial Science and Technology Leader (Innovation Team of Interface Chemistry of Efficient and Clean Utilization of Complex Mineral Resources), China; Project supported by the Co-innovation Centre for Clean and Efficient Utilization of Strategic Metal Mineral Resources, China; Project (2015CX005) supported by the Innovation Driven Plan of Central South University, China

Corresponding author: Wen-qing QIN; Tel: +86-731-88830884; E-mail: qinwenqing369@126.com
DOI: 10.1016/S1003-6326(18)64806-X

leaching of bornite was further studied by applying φ_h -pH diagram and cyclic voltammetry. This study will be helpful for better understanding of Cu-state evolution in bornite leaching process.

2 Experimental

2.1 Bornite sample

The massive bornite samples were purchased from Gaowantong Fossil Specimen Museum, Guilin, Guangxi Province, China. The samples consist of 62.26% Cu, 10.55% Fe, 23.35% S, 0.50% Pb, 0.048% Zn, 1.25% SiO₂, 0.051% MgO, 0.008% CaO and 0.32% Al₂O₃. The massive bornite samples were ground and screened to particle size of -74 μm for the leaching tests.

2.2 Enrichment culture and leaching experiments

In this study, a mixed moderately thermophilic culture consisting of the *Sulfobacillus thermosulfidoxidans* and *Acidithiobacillus caldus* was used. The microorganisms were cultured in medium consisting of 3.0 g/L (NH₄)₂SO₄, 0.1 g/L KCl, 0.5 g/L MgSO₄·7H₂O, 0.5 g/L K₂HPO₄, 0.01 g/L Ca(NO₃)₂, pH 1.6, and 0.02% yeast extract. For the bioleaching experiments, the resulting mixed culture was inoculated into 250 mL shake flasks containing 2 g of bornite and 100 mL culture medium. The initial cell concentration was 1.0×10⁷ cell/mL in solution. The abiotic experiments were conducted with the same culture medium and bornite. All leaching experiments were conducted at 160 r/min and 50 °C. The solution pH was adjusted periodically to 1.6 with diluted sulfuric acid.

2.3 Analytical techniques

Cyclic voltammetry tests were conducted with a three-electrode electrolytic cell: a chalcopyrite or bornite working electrode, a saturated Ag/AgCl reference electrode, and a graphite rod counter electrode. The electrolyte solution is the same as culture medium without yeast extract. The surface of working electrode was polished with silicon carbide papers from No. 800 to No. 3000 before each electrochemical test, and then rinsed with deionized water. Cyclic voltammetry was scanned from open circuit potential (OCP) in the positive directions with a scan rate of 20 mV/s.

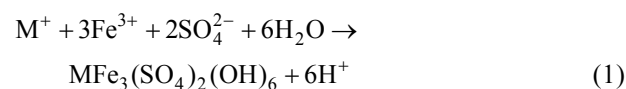
Concentrations of Fe and Cu in solution were detected via atomic absorption spectroscopy (AAS). The solution pH was measured with a pH meter (BPP-922, BELL), and the solution potentials were measured with a saturated Ag/AgCl reference electrode and a Pt electrode. At the end of each batch experiment, the leaching residues were filtered and rinsed with sulfuric acid solutions (pH 1.6), then the samples were transferred to vacuum box and dried at 40 °C before

analysis by XRD (Rigaku D/max-2000) and XPS (ESCALAB 250Xi). The details of the XPS analysis were described by WU et al [26]. Binding energy calibration was based on C 1s at 284.6 eV.

3 Results and discussion

3.1 Leaching of bornite by sterile control and microorganisms

Figure 1 shows the changes in Cu and Fe leaching rates, solution pH, and potentials during the leaching process by sterile control and microorganisms. After 30 d of leaching, 38.1% Cu and 63.9% Cu were leached from bornite by sterile control and microorganisms, respectively (Fig. 1(a)). While the corresponding leaching rates of Fe were only 14.7% and 21.8%, respectively (Fig. 1(b)). During the bioleaching of bornite, the Fe leaching rate decreased owing to the precipitation of Fe³⁺ as jarosite (Eq. (1)). The pH decline indicated that H⁺ was consumed in the entire leaching process (Fig. 1(c)). In the first 10 d of bioleaching, the solution potentials reached 470 mV due to Fe²⁺ being oxidized to Fe³⁺ by ferrous oxidizing microbial. In the following 10 d of bioleaching, the solution potential decreased from 470 to 400 mV because the oxidation rate of Fe²⁺ is lower than the consumption rate of Fe³⁺ by oxidation of bornite or precipitation of Fe³⁺, and then the solution potential stabilized at about 400 mV (Fig. 1(d)). During the sterile control leaching process, the solution potentials increased slowly and reached 370 mV after 30 d.



where M⁺ is a monovalent cation, e.g., K⁺, Na⁺, H₃O⁺, and NH₄⁺.

3.2 Characterization of bornite and leaching residues

Figure 2(a) shows the XRD pattern of bornite sample, which can be observed that peaks of orthorhombic bornite were identified. Figures 2(b) and (c) show the XRD patterns obtained for bornite leaching after 30 d. The products of bornite leaching by sterile control were CuFe₂S₃ and CuS (Fig. 2(b)). While CuFeS₂, together with less amount of S₈, was detected after leaching by microorganisms (Fig. 2(c)).

The XPS was employed to further investigate the surface compositions of bornite and leaching residues. The XPS spectrum of Cu 2p for bornite (Fig. 3(a)) shows that, the binding energy of Cu 2p_{3/2} peak is 932.0 eV, the suggested binding energy for the Cu 2p_{3/2} of bornite is 932.2–932.4 eV [2,3,27]. The binding energy (568.8 eV) of Cu LMM Auger spectrum was presented in Fig. 3(d).

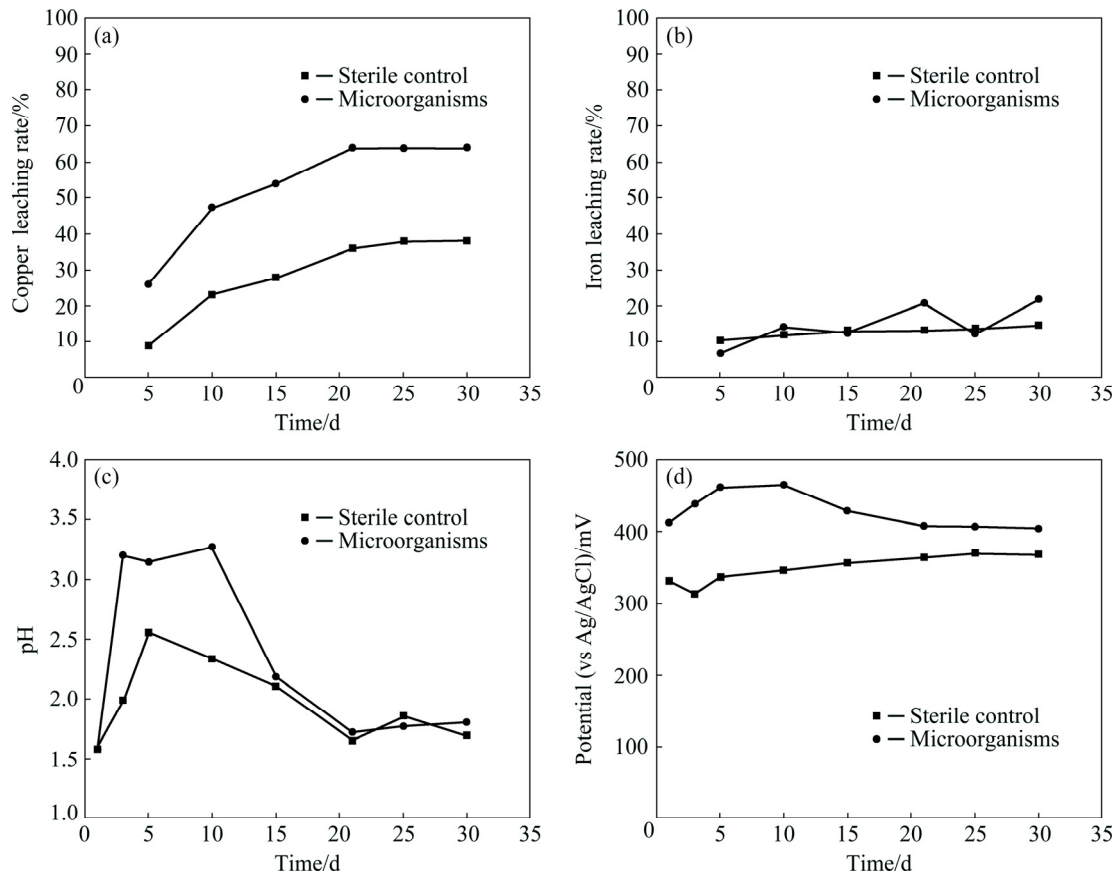


Fig. 1 Copper (a) and iron (b) leaching rates, pH (c) and potential (d) in solution during leaching of bornite

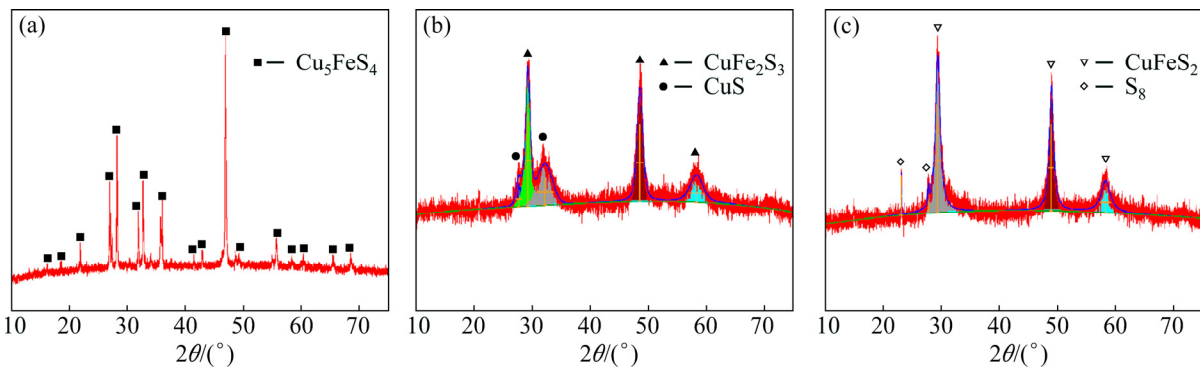


Fig. 2 XRD patterns of bornite (a), and residues leached by sterile control (b) and microorganisms (c)

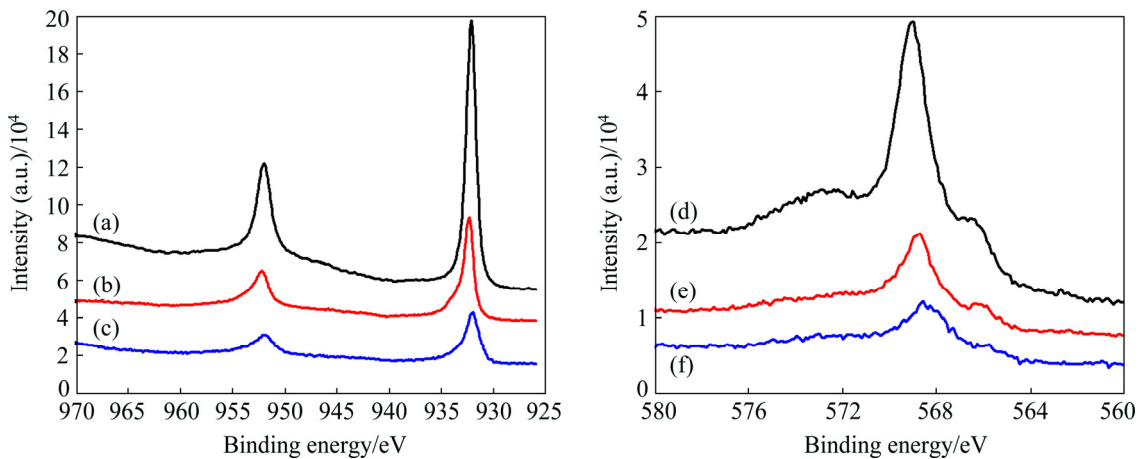


Fig. 3 XPS spectra of Cu 2p (a–c) and Cu LMM peak (d–f) of bornite (a, d), leached by sterile control (b, e) and microorganisms (c, f)

The Auger parameter value for bornite was calculated to be 1849.8 eV, which is close to the value reported by GOH et al [2]. The Cu 2p and Cu LMM spectra from relatively pure bornite are similar to those previously reported, and hence the conclusions reached earlier concerning the oxidation state of Cu in that mineral are supported [2,3]. Figure 4(a) shows the S 2p XPS spectrum of bornite which consists of two doublet peaks. The S 2p_{3/2} peak positions of two doublets are centered at 161.2 and 161.9 eV, respectively. It has been reported that the binding energy of S 2p_{3/2} of monosulfide in bornite is 161.4 eV [2]. The S 2p_{3/2} peak for the disulfide is reported to be about 161.9 eV [28,29].

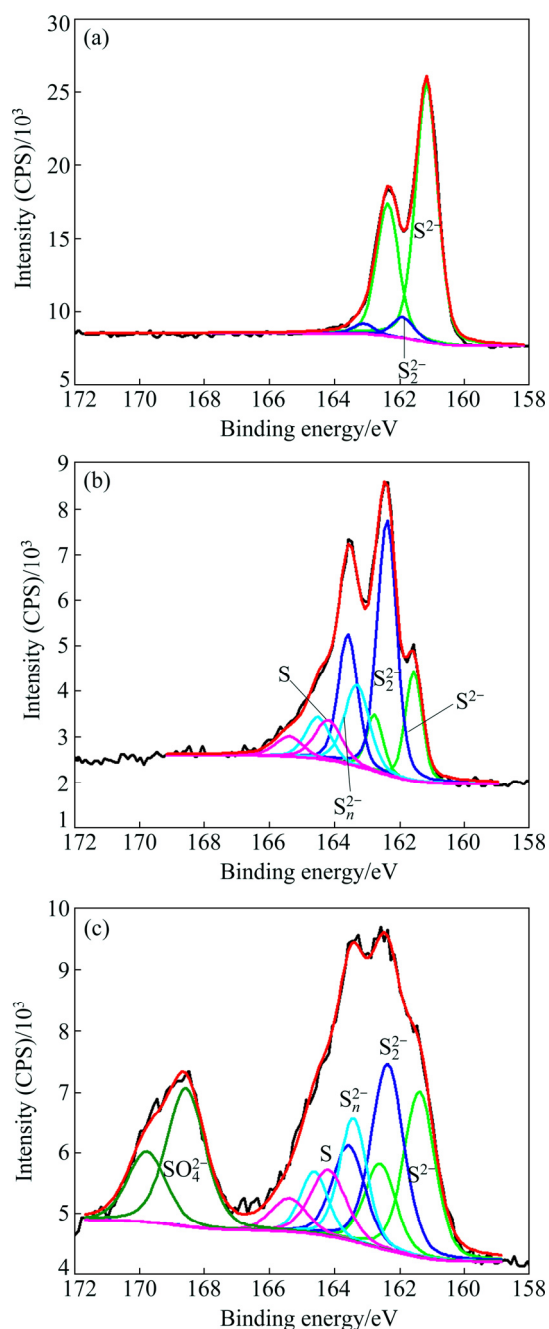


Fig. 4 XPS spectra of S 2p peak of bornite (a), leached by sterile control (b) and microorganisms (c)

The Cu 2p (Fig. 3(b)) and S 2p (Fig. 4(b)) spectra from sterile control leaching residues are similar to the photoelectron spectrum from covellite [2,30,31]. The binding energy of Cu 2p_{3/2} peak is 932.4 eV, which is in agreement with that of the CuS [32–34]. The Cu 2p spectrum is entirely consistent with a cuprous, no satellite peaks around the binding energy of 942 eV that originated from cupric were evident in the Cu 2p spectrum [35,36]. Figure 3(e) presents the Cu LMM Auger spectrum, which is centered at 568.8 eV, and the value of the Auger parameter was calculated to be 1850.2 eV, which is in the range of cuprous [2,37]. The S 2p spectrum (Fig. 4(b)) comprises four doublet peaks, and binding energies of S 2p_{3/2} were 161.6, 162.4, 163.3 and 164.2 eV, respectively. These binding energies should be assigned to the monosulfide [27,38,39], disulfide [38–40], polysulfide [38–40] and elemental sulfur [40], respectively. The binding energies of 161.6 and 162.4 eV are in agreement with what is generally found for monosulfide and disulfide of CuS [30].

Isocubanite was detected by XRD but was not detected by XPS after bornite leached by sterile control for 30 d because XRD would analyze bulk of the material, but XPS would analyze 2–5 nm surface of the material. The Cu, Fe and S molar fractions on the surface of bornite leached by sterile control were 42.99%, 6.77% and 50.24%, respectively, compared with the CuFe₂S₃ and CuS, the main leached product on the surface of bornite leached by sterile control was CuS, together with less amount of CuFe₂S₃ (Table 1).

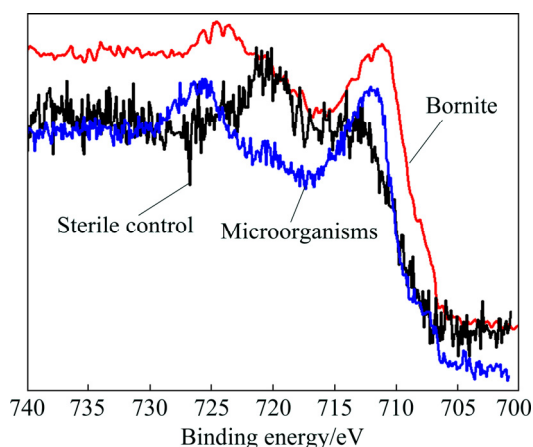
Figures 3(c) and (f) present the Cu 2p and LMM peaks of bioleaching residues, the binding energies of Cu 2p_{3/2} and Cu LMM peaks are 932.2 and 568.5 eV, respectively. After 30 d of bioleaching, cupric was absent on the surface of mineral due to the absence of satellite peak for cupric (Fig. 3(c)). Figure 4(c) shows a S 2p spectrum for bioleaching residues, five fitting peaks centered at about 161.4, 162.4, 163.4, 164.2 and 168.6 eV, which originated from the monosulfide [2,27,37], disulfide [38–40], polysulfide [38–40], elemental sulfur [40] and sulfate [28,37,40], respectively. The binding energies for S 2p_{3/2} and Cu 2p_{3/2} in chalcopyrite were 161.4 and 932.2 eV, respectively [2,26]. It can be concluded that, the most plausible cuprous species would be chalcopyrite. Simultaneously, some unidentified disulfide and polysulfide were also detected on the surface, and the disulfide and polysulfide can be referred to as “passivation” of the mineral’s complete dissolution [26]. The Cu, Fe and S molar fractions on the surface of bornite leached by microorganisms were 20.12%, 19.82% and 60.06%, respectively, compared with the Cu₅FeS₄, Cu dissolves preferentially from the bornite surface (Table 1).

Table 1 Compositions of Cu, Fe and S fractions on surface of bornite before and after leaching

Sample	Molar fraction/%			Mass fraction/%		
	Cu	Fe	S	Cu	Fe	S
Cu ₅ FeS ₄	42.15	17.74	40.11	54.05	19.99	25.96
Sterile control	42.99	6.77	50.24	57.87	8.01	34.12
Microorganisms	20.12	19.82	60.06	29.65	25.68	44.67
CuFe ₂ S ₃ *	16.67	33.33	50	23.41	41.15	35.44
CuS*	50	–	50	66.46	–	33.54
CuFeS ₂ *	25	25	50	34.63	30.43	34.94

*Theoretical value

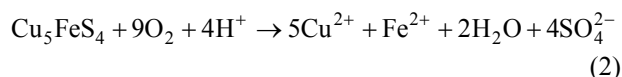
Fe 2p spectra for bornite and leaching residues are shown in Fig. 5. The Fe 2p spectrum shows that even the bornite exposed only to air was heavily oxidized. The Fe 2p peak around 711 eV can be assigned to Fe(III)—O, —OH or —OOH [32,38,40], and the presence of Fe(III)—O on the bornite surface exposed only to air was confirmed by GOH et al [2]. For the Fe 2p spectrum of sterile control leaching residues, the peak around 720 eV is the most obvious one, together with a low-intensity peak at about 712.5 eV, and these peaks would most probably be a Cu L₂M_{2,3}M_{2,3} peak [3,37] and Cu L₃M_{2,3}M_{2,3} [41]. For the Fe 2p spectrum of bioleaching residues, the peak near 712 eV can be assigned to jarosite, which is in agreement with S 2p spectrum shown in Fig. 4(c).

**Fig. 5** XPS spectra of Fe 2p peak of bornite, leached by sterile control and microorganisms

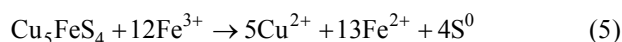
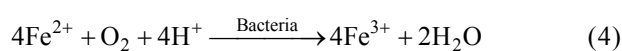
3.3 Discussion

As previously mentioned, H⁺ was consumed in the whole leaching process. It was well established in the literature that Cu₅FeS₄ was leached by the dissolved O₂ and H⁺ via Eq. (2) [14,16]. Alternatively, ZIES et al [42] stated that the H⁺ firstly attacked the Cu₅FeS₄, which was converted to CuS and Cu₂S, and Fe²⁺ and H₂S were formed at the same time. Moreover, Fe²⁺, Cu₂S or CuS, and H₂S could react and form CuFeS₂. CuS and CuFeS₂ were detected by XRD in the sterile control and

microorganisms leaching residues, respectively. But Cu₂S was not detected because it was easily oxidized. Figure 1(d) also shows that in the sterile control leaching process, the increase of Fe²⁺ concentration in leaching solution caused the decrease of solution potential in first 3 d. Because the solution potential in leaching solution is mainly decided by the ratio of Fe³⁺/Fe²⁺ according to the Nernst equation (Eq. (3)) [43,44]. In the bioleaching process, Cu₅FeS₄ was firstly leached by O₂ and H⁺, and then the oxidation of Fe²⁺ to Fe³⁺ by microorganisms caused the increase of solution potential (Eq. (4)). Simultaneously, Cu₅FeS₄ was leached by Fe³⁺ via Eq. (5). According to Figs. 1(a) and (d), it can be concluded that the bornite was more likely to be leached at high solution potential.



$$\varphi = \varphi^\ominus + \frac{RT}{F} \ln \frac{[\text{Fe}^{3+}]}{[\text{Fe}^{2+}]} \quad (3)$$



The φ_h -pH diagram for Cu-Fe-S-H₂O system at 50 °C was calculated by HSC 6.0, as shown in Fig 6(a). There are two stable areas for Cu₅FeS₄. It can be seen that Cu₅FeS₄ can transform into Cu₂S, CuFeS₂ and CuS. There may be two paths for the oxidation of CuFeS₂ to Cu²⁺: at low pH, CuFeS₂→CuS→Cu₂S→Cu²⁺; at high pH, CuFeS₂→Cu₅FeS₄→(CuS)→Cu₂S→Cu²⁺.

Figure 6(b) shows the cyclic voltammogram of Cu₅FeS₄. One anodic peak (A₁) and two cathodic peaks (C₁ and C₂) were detected. Anodic peak A₁ represented the oxidation of Cu₅FeS₄. Several authors assumed that Cu₅FeS₄ oxidation proceeded by stepwise breakdown via Eqs. (6) and (7), and the overall reaction of oxidation of Cu₅FeS₄ was presented as Eq. (8) [10–12]. Alternatively, Cu₅FeS₄ could be oxidized to CuS in acid media (Eq. (9)) [9,12]. Cathodic peak C₁ represented the reduction of Fe³⁺ to Fe²⁺ (Eq. (10)) [7], and/or reduction of Cu²⁺ and CuS to Cu₂S (Eq. (11)) [8]. The reduction of

Cu₅FeS₄ to Cu₂S occurred at peak C₂ (Eq. (12)) [8,27].

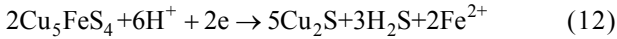
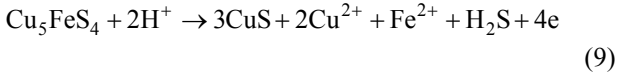
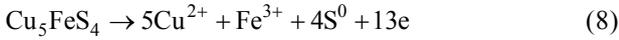
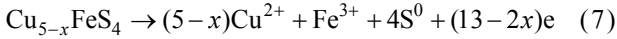
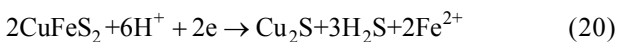
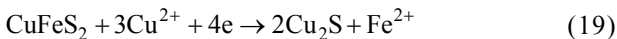
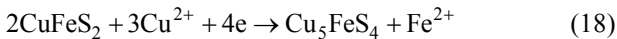
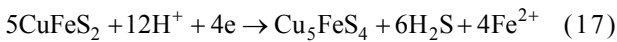
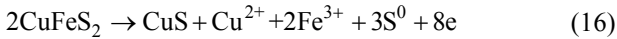
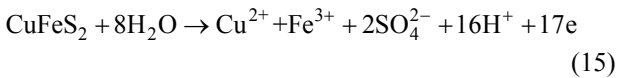
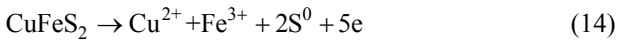
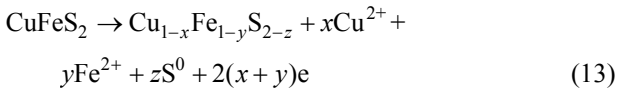


Figure 6(c) shows the cyclic voltammogram of CuFeS₂. Two anodic peaks (A₁' and A₂') and three cathodic peaks (C₁', C₂' and C₃') were detected. Peak A₁' should be assigned to the preferential dissolution of Fe from the CuFeS₂ according to Eq. (13) [8,37]. Peak A₂' is related to the dissolution of CuFeS₂ to Cu²⁺, Fe³⁺, S⁰ and/or SO₄²⁻ [8,45,46], as shown in Eqs. (14) and (15). Especially, CuFeS₂ can be oxidized to CuS via Eq. (16) [9,37]. Peak C₁' is similar to C₁, which represents the reduction of Fe³⁺ to Fe²⁺ (Eq. (10)), and/or reduction of Cu²⁺ and CuS to Cu₂S (Eq. (11)). According to Refs. [7,8,27], the reduction of CuFeS₂ shown in Eqs. (17)–(19) took place at peak C₂'. The Cu₅FeS₄ was also detected on the surface after electrochemical oxidation of CuFeS₂ in the potential window of 0.75 to 0.90 V [9]. The reduction of Cu₅FeS₄ and CuFeS₂ to Cu₂S occurred at peak C₃' via Eqs. (12) and (20) [7,8,27], respectively.



ZIES et al [42] reported that when CuFeS₂ was added into the solution containing Cu²⁺, CuFeS₂ could react with Cu²⁺ and be transformed into Cu₂S and/or CuS (Eqs. (21) and (22)). The formed CuS could further convert into Cu₂S by Eq. (23). Cu₅FeS₄ could also convert into Cu₂S and/or CuS (Eqs. (24) and (25)). The Cu₂S was not detected by XRD in our experiments because the Cu₂S was very easily oxidized. Furthermore, the isocubanite was detected in sterile control leaching.

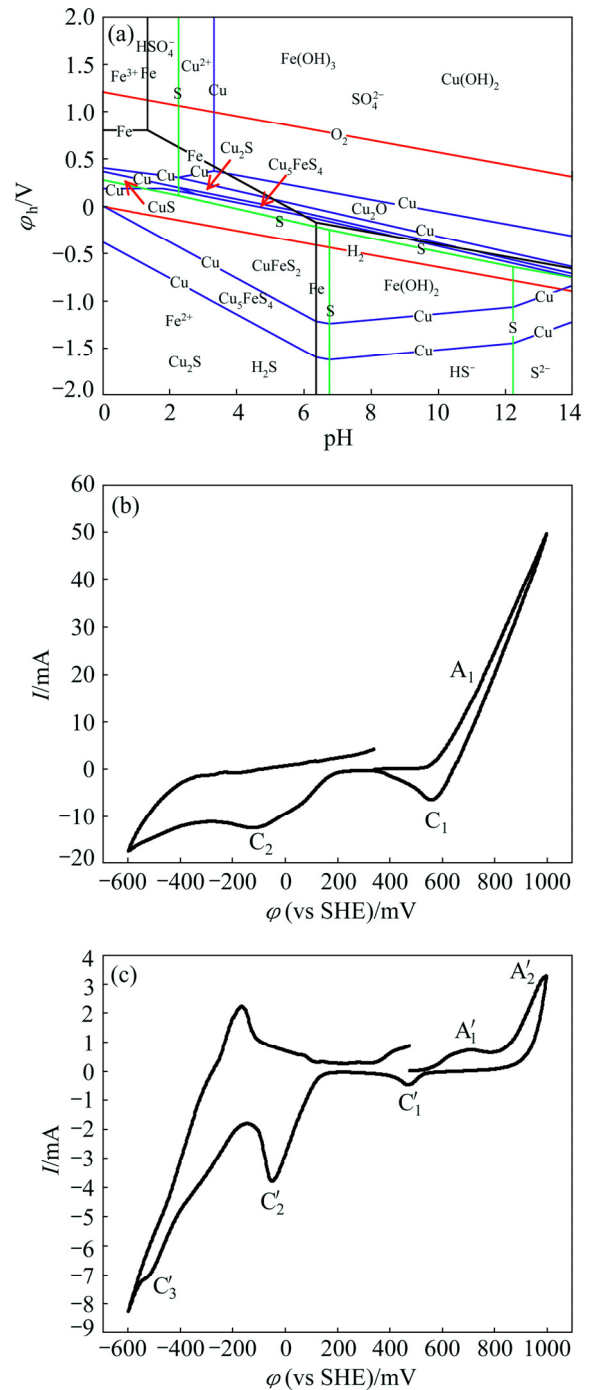
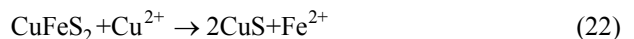
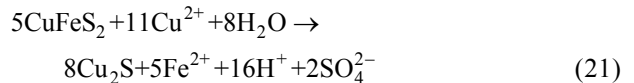
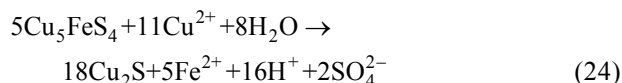


Fig. 6 ϕ_h -pH diagram for Cu-Fe-S-H₂O system at 50 °C, $a_{\text{Cu}}=0.1$ mol/L, $a_{\text{Fe}}=0.1$ mol/L, $a_{\text{S}}=0.5$ mol/L and 323 K (a), and cyclic voltammograms of bornite ($\phi_{\text{OCP}}=340$ mV) (b) and chalcopyrite ($\phi_{\text{OCP}}=475$ mV) (c) electrodes

ELLIOT and WATLING [47] reported that CuFe₂S₃ can be transformed into CuFeS₂ via Eq. (26).





In summary, Cu_5FeS_4 can be transformed into Cu_2S , CuFeS_2 and CuS . There may be two paths for the oxidation of CuFeS_2 to Cu^{2+} : 1) at low pH, $\text{CuFeS}_2 \rightarrow \text{CuS} \rightarrow \text{Cu}_2\text{S} \rightarrow \text{Cu}^{2+}$; and 2) at high pH, $\text{CuFeS}_2 \rightarrow \text{Cu}_5\text{FeS}_4 \rightarrow (\text{CuS}) \rightarrow \text{Cu}_2\text{S} \rightarrow \text{Cu}^{2+}$.

4 Conclusions

1) Leaching experiment showed that the Cu leaching rates for the bornite were 63.9% and 38.1% by microorganisms and sterile control, respectively; in comparison, only 21.8% Fe and 14.7% Fe were leached by microorganisms and sterile control, respectively. This means that bornite was more likely to be leached at high redox potential.

2) Intermediary sulfides, such as isocubanite, covellite, chalcopyrite, disulfide, and polysulfide, were formed during bornite dissolution. The Cu 2p photoelectron spectrum revealed that the valence of copper in bornite and intermediary sulfide formed in the dissolution of bornite is +1.

3) Bornite can be transformed into chalcocite, chalcopyrite, and covellite. There may be two paths for oxidation of chalcopyrite to Cu^{2+} : 1) at low pH, $\text{CuFeS}_2 \rightarrow \text{CuS} \rightarrow \text{Cu}_2\text{S} \rightarrow \text{Cu}^{2+}$; and 2) at high pH, $\text{CuFeS}_2 \rightarrow \text{Cu}_5\text{FeS}_4 \rightarrow (\text{CuS}) \rightarrow \text{Cu}_2\text{S} \rightarrow \text{Cu}^{2+}$.

References

- [1] van der LAAN G, PATTRICK R A D, CHARNOCK J M, GRGURIC B A. Cu L 2,3 X-ray absorption and the electronic structure of nonstoichiometric Cu_5FeS_4 [J]. *Physical Review B*, 2002, 66(4): 045104.
- [2] GOH S W, BUCKLEY A N, LAMB R N, ROSENBERG R A, MORAN D. The oxidation states of copper and iron in mineral sulfides, and the oxides formed on initial exposure of chalcopyrite and bornite to air [J]. *Geochimica et Cosmochimica Acta*, 2006, 70(9): 2210–2228.
- [3] HARMER S L, PRATT A R, NESBITT H W, FLEET M E. Reconstruction of fracture surfaces on bornite [J]. *Canadian Mineralogist*, 2005, 43: 1619–1630.
- [4] BORGHERESI M, BERNARDINI G P, CIPRIANI C, DI BENEDETTO F, ROMANELLI M. Electron paramagnetic resonance and electron spin echo spectroscopy study of natural bornite [J]. *Mineralogy and Petrology*, 2005, 85(1–2): 3–18.
- [5] MIKHLIN Y, TOMASHEVICH Y, TAUSON V, VYALIKH D, MOLODTSOV S, SZARGAN R. A comparative X-ray absorption near-edge structure study of bornite, Cu_5FeS_4 , and chalcopyrite, CuFeS_2 [J]. *Journal of Electron Spectroscopy and Related Phenomena*, 2005, 142(1): 83–88.
- [6] BEVILAQUA D, DIÉZ-PEREZ I, FUGIVARA C S, SANZ F, GARCIA O, BENEDETTI A V. Characterization of bornite (Cu_5FeS_4) electrodes in the presence of the bacterium *Acidithiobacillus ferrooxidans* [J]. *Journal of the Brazilian Chemical Society*, 2003, 14(4): 637–644.
- [7] QIN Wen-qing, YANG Cong-ren, LAI Shao-shi, WANG Jun, LIU Kai, ZHANG Bo. Bioleaching of chalcopyrite by moderately thermophilic microorganisms [J]. *Bioresource Technology*, 2013, 129: 200–208.
- [8] LIANG Chang-li, XIA Jin-lan, YANG Yi, NIE Zhen-yuan, ZHAO Xiao-juan, ZHENG Lei, MA Chen-yan, ZHAO Yi-dong. Characterization of the thermo-reduction process of chalcopyrite at 65 °C by cyclic voltammetry and XANES spectroscopy [J]. *Hydrometallurgy*, 2011, 107(1–2): 13–21.
- [9] MAJUSTE D, CIMINELLI V S T, OSSEO-ASARE K, DANTAS M S S, MAGALHÃES-PANIAGO R. Electrochemical dissolution of chalcopyrite: Detection of bornite by synchrotron small angle X-ray diffraction and its correlation with the hindered dissolution process [J]. *Hydrometallurgy*, 2012, 111: 114–123.
- [10] PRICE D C, CHILTON J P. The anodic reactions of bornite in sulphuric acid solution [J]. *Hydrometallurgy*, 1981, 7(1): 117–133.
- [11] PRICE D C, CHILTON J P. The electroleaching of bornite and chalcopyrite [J]. *Hydrometallurgy*, 1980, 5(4): 381–394.
- [12] ARCE E M, GONZÁLEZ I. A comparative study of electrochemical behavior of chalcopyrite, chalcocite and bornite in sulfuric acid solution [J]. *International Journal of Mineral Processing*, 2002, 67(1–4): 17–28.
- [13] PESIC B, OLSON F A. Dissolution of bornite in sulfuric acid using oxygen as oxidant [J]. *Hydrometallurgy*, 1984, 12(2): 195–215.
- [14] BEVILAQUA D, ACCIARI H A, ARENA F A, BENEDETTI A V, FUGIVARA C S, TREMILIOSI FILHO G, GARCIA JÚNIOR O. Utilization of electrochemical impedance spectroscopy for monitoring bornite (Cu_5FeS_4) oxidation by *Acidithiobacillus ferrooxidans* [J]. *Minerals Engineering*, 2009, 22(3): 254–262.
- [15] ZHAO Hong-bo, HU Ming-hao, LI Yi-ni, ZHU Shan, QIN Wen-qing, QIU Guan-zhou, WANG Jun. Comparison of electrochemical dissolution of chalcopyrite and bornite in acid culture medium [J]. *Transactions of Nonferrous Metals Society of China*, 2015, 25(1): 303–313.
- [16] BEVILAQUA D, GARCIA O Jr, TUOVINEN O H. Oxidative dissolution of bornite by *Acidithiobacillus ferrooxidans* [J]. *Process Biochemistry*, 2010, 45(1): 101–106.
- [17] BEVILAQUA D, ACCIARI H A, BENEDETTI A V, FUGIVARA C S, TREMILIOSI FILHO G, GARCIA O Jr. Electrochemical noise analysis of bioleaching of bornite (Cu_5FeS_4) by *Acidithiobacillus ferrooxidans* [J]. *Hydrometallurgy*, 2006, 83(1): 50–54.
- [18] ZHAO Hong-bo, WANG Jun, HU Ming-hao, QIN Wen-qing, ZHANG Yan-sheng, QIU Guan-zhou. Synergistic bioleaching of chalcopyrite and bornite in the presence of *Acidithiobacillus ferrooxidans* [J]. *Bioresource Technology*, 2013, 149: 71–76.
- [19] WANG Jun, TAO Lang, ZHAO Hong-bo, HU Ming-hao, ZHENG Xi-hua, PENG Hong, GAN Xiao-wen, XIAO Wei, CAO Pan, QIN Wen-qing, QIU Guan-zhou, WANG Dian-zuo. Cooperative effect of chalcopyrite and bornite interactions during bioleaching by mixed moderately thermophilic culture [J]. *Minerals Engineering*, 2016, 95: 116–123.
- [20] FERRAZ L F C, VERDE L C L, REIS F C, ALEXANDRINO F, FELÍCIO A P, NOVO M T M, GARCIA O Jr, OTTOBONI L M M. Gene expression modulation by chalcopyrite and bornite in *Acidithiobacillus ferrooxidans* [J]. *Archives of Microbiology*, 2010, 192(7): 531–540.
- [21] FELÍCIO A P, DE OLIVEIRA E, ODENA M A, GARCIA O Jr, BERTOLINI M C, FERRAZ L F C, OTTOBONI L M M, NOVO M T M. Differential proteomic analysis of *Acidithiobacillus ferrooxidans* cells maintained in contact with bornite or chalcopyrite: Proteins involved with the early bacterial response [J]. *Process Biochemistry*, 2011, 46(3): 770–776.
- [22] VILCÁEZ J, SUTO K, INOUE C. Bioleaching of chalcopyrite with thermophiles: Temperature-pH-ORP dependence [J]. *International*

- Journal of Mineral Processing, 2008, 88(1–2): 37–44.
- [23] XIONG Xian-xue, GU Guo-hua, BAN Jin-rong, LI Shuang-ke. Bioleaching and electrochemical property of marmatite by *Sulfobacillus thermosulfidooxidans* [J]. Transactions of Nonferrous Metals Society of China, 2015, 25(9): 3103–3110.
- [24] CASTRO C, DONATI E R. Improving zinc recovery by thermoacidophilic archaeon *Acidianus copahuensis* using tetrathionate [J]. Transactions of Nonferrous Metals Society of China, 2016, 26(11): 3004–3014.
- [25] LIU Hong-chang, XIA Jin-lan, NIE Zhen-yuan, MA Ya-long, MA Chen-yan, ZHENG Lei, HONG Cai-hao, ZHAO Yi-dong. Iron L-edge and sulfur K-edge XANES spectroscopy analysis of pyrite leached by *Acidianus manzaensis* [J]. Transactions of Nonferrous Metals Society of China, 2015, 25(7): 2407–2414.
- [26] WU Shi-fa, YANG Cong-ren, QIN Wen-qing, JIAO Fen, WANG Jun, ZHANG Yan-sheng. Sulfur composition on surface of chalcopyrite during its bioleaching at 50 °C [J]. Transactions of Nonferrous Metals Society of China, 2015, 25(12): 4110–4118.
- [27] NAVA D, GONZÁLEZ I, LEINEN D, RAMOS-BARRADO J R. Surface characterization by X-ray photoelectron spectroscopy and cyclic voltammetry of products formed during the potentiostatic reduction of chalcopyrite [J]. Electrochimica Acta, 2008, 53(14): 4889–4899.
- [28] KLAUBER C, PARKER A, van BRONSWIJK W, WATLING H. Sulphur speciation of leached chalcopyrite surfaces as determined by X-ray photoelectron spectroscopy [J]. International Journal of Mineral Processing, 2001, 62(1–4): 65–94.
- [29] KLAUBER C. Fracture-induced reconstruction of a chalcopyrite (CuFeS₂) surface [J]. Surface and Interface Analysis, 2003, 35(5): 415–428.
- [30] GOH S W, BUCKLEY A N, LAMB R N. Copper(II) sulfide? [J]. Minerals Engineering, 2006, 19(2): 204–208.
- [31] KUNDU M, HASEGAWA T, TERABE K, AONO M. Effect of sulfurization conditions on structural and electrical properties of copper sulfide films [J]. Journal of Applied Physics, 2008, 103(7): 073523.
- [32] BRION D. Study by photoelectron-spectroscopy of surface degradation of FeS₂, CuFeS₂, ZnS and PbS exposed to air and water [J]. Applied Surface Science, 1980, 5(2): 133–152.
- [33] NAKAI I, SUGITANI Y, NAGASHIMA K, NIWA Y. X-ray photoelectron spectroscopic study of copper minerals [J]. Journal of Inorganic and Nuclear Chemistry, 1978, 40(5): 789–791.
- [34] PERRY D L, TAYLOR J A. X-ray photoelectron and Auger spectroscopic studies of Cu₂S and CuS [J]. Journal of Materials Science Letters, 1986, 5(4): 384–386.
- [35] YIN M, WU C K, LOU Y B, BURDA C, KOBERSTEIN J T, ZHU Y M, O'BRIEN S. Copper oxide nanocrystals [J]. Journal of the American Chemical Society, 2005, 127(26): 9506–9511.
- [36] CHUSUEI C C, BROOKSHIER M A, GOODMAN D W. Correlation of relative X-ray photoelectron spectroscopy shake-up intensity with CuO particle size [J]. Langmuir, 1999, 15(8): 2806–2808.
- [37] GHAREMANINEZHAD A, DIXON D G, ASSELIN E. Electrochemical and XPS analysis of chalcopyrite (CuFeS₂) dissolution in sulfuric acid solution [J]. Electrochimica Acta, 2013, 87: 97–112.
- [38] ACRES R G, HARMER S L, BEATTIE D A. Synchrotron XPS studies of solution exposed chalcopyrite, bornite, and heterogeneous chalcopyrite with bornite [J]. International Journal of Mineral Processing, 2010, 94(1–2): 43–51.
- [39] ACRES R G, HARMER S L, BEATTIE D A. Synchrotron XPS, NEXAFS, and ToF-SIMS studies of solution exposed chalcopyrite and heterogeneous chalcopyrite with pyrite [J]. Minerals Engineering, 2010, 23(11–13): 928–936.
- [40] HARMER S L, THOMAS J E, FORNASIERO D, GERSON A R. The evolution of surface layers formed during chalcopyrite leaching [J]. Geochimica et Cosmochimica Acta, 2006, 70(17): 4392–4402.
- [41] SCHÖN G. High resolution Auger electron spectroscopy of metallic copper [J]. Journal of Electron Spectroscopy and Related Phenomena, 1972, 1(4): 377–387.
- [42] ZIES E G, ALLE E T, MERWIN H E. Some reactions involved in secondary copper sulphide enrichment [J]. Economic Geology, 1916, 11(5): 407–503.
- [43] KHOSHKHO M, DOPSON M, SHCHUKAREV A, SANDSTRÖM Å. Chalcopyrite leaching and bioleaching: An X-ray photoelectron spectroscopic (XPS) investigation on the nature of hindered dissolution [J]. Hydrometallurgy, 2014, 149: 220–227.
- [44] ZHAO Hong-bo, WANG Jun, YANG Cong-ren, HU Ming-hao, GAN Xiao-wen, TAO Lang, QIN Wen-qing, QIU Guan-zhou. Effect of redox potential on bioleaching of chalcopyrite by moderately thermophilic bacteria: An emphasis on solution compositions [J]. Hydrometallurgy, 2015, 151: 141–150.
- [45] GÓMEZ C, FIGUEROA M, MUÑOZ J, BLÁZQUEZ M L, BALLESTER A. Electrochemistry of chalcopyrite [J]. Hydrometallurgy, 1996, 43(1–3): 331–344.
- [46] LÓPEZ-JUÁREZ L A, GUTIÉRREZ-ARENAS N, RIVERA-SANTILLAN R E. Electrochemical behavior of massive chalcopyrite bioleached electrodes in presence of silver at 35 °C [J]. Hydrometallurgy, 2006, 83(1–4): 63–68.
- [47] ELLIOT A D, WATLING H R. Chalcopyrite formation through the metathesis of pyrrhotite with aqueous copper [J]. Geochimica et Cosmochimica Acta, 2011, 75(8): 2103–2118.

斑铜矿在 50 °C 浸出过程中的铜物相转化

杨聪仁, 焦芬, 覃文庆

中南大学 资源加工与生物工程学院, 长沙 410083

摘要: 研究斑铜矿在 50 °C 的混合中等嗜热微生物浸出。通过 XRD 和 XPS 表征在斑铜矿浸出过程中形成的中间产物, 并利用 ϕ_h -pH 图和循环伏安曲线进一步分析斑铜矿浸出过程中铜状态的转化。结果表明: 较高的溶液(氧化还原)电位更有利于斑铜矿的浸出; 在斑铜矿的浸出过程中可能形成方黄铜矿、铜蓝、黄铜矿以及二硫化物和多硫化物等中间产物; Cu 2p 光电子能谱显示, 斑铜矿和中间产物中铜的价态均为+1。斑铜矿和黄铜矿之间可以相互转化, 并且两者都可以进一步转化为铜蓝和/或辉铜矿。

关键词: 浸出; 斑铜矿; 黄铜矿; 铜蓝; 铜物相转化

(Edited by Wei-ping CHEN)